

# GUARD: Toward a Compromise between Traditional Control and Learning for Safe Robot Systems

Johannes A. Gaus<sup>1</sup>, Junheon Yoon<sup>2</sup>, Woo-Jeong Baek<sup>3</sup>, Seungwon Choi<sup>4</sup>, Suhan Park<sup>5</sup>, Jaeheung Park<sup>2</sup>

**Abstract**—This paper presents the framework GUARD (Guided robot control via Uncertainty attribution and probAbilistic kernel optimization for Risk-aware Decision making) that combines traditional control with an uncertainty-aware perception technique using active learning with real-time capability for safe robot collision avoidance. By doing so, this manuscript addresses the central challenge in robotics of finding a reasonable compromise between traditional methods and learning algorithms to foster the development of safe, yet efficient and flexible applications. By unifying a reactive model predictive countouring control (RMPCC) with an Iterative Closest Point (ICP) algorithm that enables the attribution of uncertainty sources online using active learning with real-time capability via a probabilistic kernel optimization technique, GUARD inherently handles the existing ambiguity of the term *safety* that exists in robotics literature. Experimental studies indicate the high performance of GUARD, thereby highlighting the relevance and need to broaden its applicability in future.

## I. INTRODUCTION

Developing safe and flexible robot applications is a central, yet open issue in robotics. One major difficulty arises due to the challenge to develop systems that are sufficiently explainable to verify safety, and enable the use of efficient learning methods. Thus, a suitable compromise must be found such that safety, that requires explainability, can be evaluated while preserving the benefits of learning. While end-to-end learning like in ([1], [2], [3]) have led to promising results regarding their efficiency, their black-box character causes a burden on assessing safety. A second challenge lies in the ambiguity of the safety definitions in the different subdomains. Robotic systems employ methods from control, perception, and/or state estimation. Especially, the respective assumptions that must be met (e.g., control barrier functions (CBFs) in traditional control, registration accuracy in perception,...) are formulated in a domain-specific manner. However, the relationship between these requirements is often not known. For example, it remains unclear how the perception parameters affect the robot control performance in the context of safety. To complement traditional techniques with learning in a safe and efficient manner, this paper contends that safety is evaluated inversely by the *uncertainty*.

<sup>1</sup> Hertie Institute for Clinical Brain Research & Center for Integrative Neuroscience, University of Tübingen, Germany.

<sup>2</sup> Department of Intelligence and Information, Graduate School of Convergence Science and Technology, Seoul National University, Republic of Korea.

<sup>3</sup> Artificial Intelligence Institute (AIIS), Seoul National University, Republic of Korea.

<sup>4</sup> Department of Naval Architecture and Ocean Engineering, Seoul National University, Republic of Korea.

<sup>5</sup> School of Robotics, Kwangwoon University, Seoul, Republic of Korea.

Thus, the uncertainty is treated as the key measure for safety evaluation. The uncertainty reflects the possible deviation of a quantity and is expressed as a probability. Logically, the absence of uncertainties (uncertainty = 0) ensures safety: In case all system variables are known with perfect accuracy at each time step, dangerous situations can be avoided by introducing risk-avoiding measures in time. This paper suggests GUARD to combine reactive model predictive contouring control (RMPCC) from prior work in [4] that ensures smooth evasive movements with uncertainty-aware ICP. By further actively adapting the kernel parameters via our previous work in [5], robustness is achieved. This unification adapts the safety conditions of the CBFs in the RMPCC by referring to the perception uncertainties. Practically, more conservative robot movements are generated in case of high perception uncertainties while maximizing the efficiency for negligible uncertainties. The real-time capability (100Hz) enables to handle sudden occurrence of obstacles or unexpected disturbances.

*a) Related Work:* Classical path following can be split into time-parameterized planners/trackers and path-parameterized MPC. The former optimize a time-indexed trajectory that a low-level controller tracks [6]–[11]; the latter optimizes progress along a spatial path to gain temporal flexibility and real-time reactivity evaluated on cars, UAVs, and manipulators [12], [13]. For safety, artificial potential fields have been widely used, while CBFs yield forward-invariance guarantees and typically less intrusive avoidance [14], [15]. RMPCC combines path-parameterized MPC with CBFs and achieves high servo rates via Jacobian linearization and Gauss–Newton/SQP [4]. On the perception side, ICP remains the workhorse for point-cloud registration [16], [17]. Uncertainty has been analyzed via closed-form covariances [18] and their limitations [19], learned covariance predictors (CELLO-3D) [20], and probabilistic/multi-modal variants (e.g., Stein-ICP) [21]. However, most pipelines quantify *how much* uncertainty exists but not *why*. Concept-based explanations as TCAV [22] with point-cloud encoders (PointNet/DGCNN) [23], [24] enable human-interpretable attribution. Recent post-hoc attribution for ICP exists but is computationally heavy and not integrated with control [25]. Probabilistic Kernel Optimization (PKO) adapts robust kernels by matching model/data inlier distributions to improve registration robustness [5].

**Contribution.** GUARD differs by (i) attaching per-concept, calibrated attributions to ICP uncertainty and (ii) feeding these uncertainties into RMPCC to adapt safety margins

online while preserving real-time performance, bridging perception failures to control guarantees.

## II. PRELIMINARIES AND PRIOR WORK

**Iterative Closest Point (ICP) Algorithm** ICP estimates the rigid motion  $T = (R, t) \in SE(3)$  that aligns a source point cloud to a target cloud by alternating correspondence assignment and a small weighted least-squares update. In the point-to-plane variant [16], each iteration minimizes residuals of the form

$$r_i = \mathbf{n}_i^\top (R\mathbf{p}_i + t - \mathbf{q}_i).$$

The per-iteration residual set  $\{r_i\}$ , inlier counts, and overlap proxies provide both the pose estimate and rich cues about the scene (e.g., occlusion, poor overlap, dynamic objects).

### Probabilistic Kernel Optimization (PKO)

Our previous work [5] uses above residuals to adapt the robust kernel parameters by matching an inlier distribution with the empirical residual. To be specific, PKO refers to the iteratively reweighted least squares (IRLS) algorithm that employs a weighting scheme for the residuals by assigning smaller weights to outliers, thereby minimizing their influence on the optimization. PKO enhances the robustness as follows: For the IRLS weight  $w(r; c)$  with the scaling parameter  $c$  of the robust kernel, a model-based inlier probability  $P_{\text{model}}(\text{inlier} | r, c) = w(r; c)/Z_w$ , and a data-based inlier probability  $P_{\text{data}}(\text{inlier} | r)$  from a short window of recent residual magnitudes is defined. At each IRLS iteration,  $c$  is adapted via the Jensen-Shannon divergence  $JS$ :

$$c^* = \arg \min_c JS\left(P_{\text{data}}(\cdot) \parallel P_{\text{model}}(\cdot | c)\right).$$

This aligns the effective inlier boundary with the sensor data reflecting the actual state. With the improving alignment,  $c^*$  decreases, reproducing a graduated-nonconvexity behavior. PKO improves the tolerance against initialization uncertainties, sensor noise and partial overlaps.

### TCAV-GPC for uncertainty attribution for ICP

The lack of interpretability in residual-driven adaptation is addressed by integrating the technique of Testing with Concept Activation Vectors (TCAV) [22]. The perception is performed via RGB-D frames that are processed with ICP. With the obtained point clouds, TCAV extracts expressive features via a pretrained model like Dynamic Graph CNN (DGCNN) or a PointNet approach [23], [24]. For the embedding  $e_k = f_\theta(P_k)$  generated by the encoder corresponding to the point cloud  $P_k$ , a feature vector

$$\phi_k = [e_k] \in \mathbb{R}^d$$

is formed. By training a multi-class Gaussian Process Classifier (GPC) with these vectors on artificially perturbed data, the goal is to classify  $\phi_k$  in three semantic uncertainty concepts

$$\mathcal{C} = \{\text{sensor noise, pose error, partial overlap}\}.$$

At test time the GPC yields calibrated posteriors

$$\pi_k(c) = p(c | \phi_k, \mathcal{D}), \quad c \in \mathcal{C}, u_k = -\sum_{c \in \mathcal{C}} \pi_k(c) \log \pi_k(c),$$

where  $u_k$  summarizes overall predictive uncertainty. In practice,  $\pi_k(c)$  is computed via a standard multi-class GP link

with a Laplace approximation or Monte Carlo samples of the latent scores. Sampling from the GPC posterior provides both per-concept attribution scores  $\{\pi_k(c)\}_{c \in \mathcal{C}}$  and calibrated uncertainty estimates  $u_k$ . This analysis inspired by TCAV in [22] in the encoder space provides

$$s_c(e_k) = \nabla_e g_c(e) \Big|_{e=e_k}^\top \mathbf{v}_c,$$

where  $g_c$  is the pre-link class score and  $\mathbf{v}_c$  is the concept activation vector for concept  $c$ . This enables the system both to measure *how* uncertain a registration is ( $u_k$ ) and to explain *why* (via the dominant concept  $c_k^* = \arg \max_c \pi_k(c)$ ). These results are referred to as a threshold for the PKO adaptation.

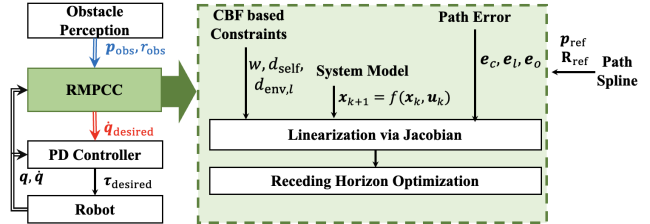


Fig. 1: Schematic overview of RMPCC taken and adapted from [4]. Assuming a perfectly accurate perception, RMPCC proposes a controller that considers CBF constraints.

### Reactive Model Predictive Contouring Control (RMPCC)

Our prior work [4] presents RMPCC shown in Figure 1 that follows a reference path with CBFs. The robot path is parameterized by a path parameter  $s \in [0, 1]$ , formalized via a position spline  $p_r(s) \in \mathbb{R}^3$  and an orientation curve  $R_r(s) \in SO(3)$ . For the robot joint configuration  $q \in \mathbb{R}^n$ , the end-effector pose  $p_{ee}(q)$  and  $R_{ee}(q)$ , RMPCC refers to a surrogate path-progress state  $(s, v_s)$  with discrete dynamics. For the robot state and control input

$$x_k = [q_k^\top \quad s_k \quad v_{s,k}]^\top, \quad u_k = [\dot{q}_k^\top \quad \dot{v}_{s,k}]^\top,$$

the controller minimizes tracking error and control effort over a horizon  $N$ :

$$J = L_f(x_N) + \sum_{k=1}^{N-1} L(x_k, u_k, u_{k-1}), \quad (1)$$

with stage cost

$$\begin{aligned} L = & \underbrace{w_c \|e_c\|^2 + w_l \|e_l\|^2 + w_{v_s} (v_{\text{des}} - v_{s,k})^2}_{\text{tracking}} \\ & + \underbrace{w_o \|\text{Log}(R_r^\top R_{ee})\|^2}_{\text{orientation}} \\ & + \underbrace{w_{\dot{q}} \|\dot{q}_k\|^2 + w_{\Delta\dot{q}} \|\Delta\dot{q}_k\|^2 + w_{\dot{v}_{s,k}} \dot{v}_{s,k}^2}_{\text{regularization}}, \end{aligned} \quad (2)$$

Here,  $e = p_r(s_k) - p_{ee}(q_k)$  is split into contouring and lag error using the local path tangent,  $\Delta\dot{q}_k = \dot{q}_k - \dot{q}_{k-1}$  (with  $\Delta\dot{q}_1 = 0$ ), and  $\text{Log}(\cdot)$  denotes the matrix logarithm on  $SO(3)$ . Safety is considered via CBFs on (i) kinematic singularities, (ii) self-collision, and (iii) environment collision. The algorithm proposes barrier functions  $h(q) \geq 0$

$$h_{\text{sing}}(q) = \mu(q) - \varepsilon_{\text{sing}}, \quad (3)$$

$$\mu(q) = \sqrt{\det(J_{ee}(q) J_{ee}(q)^\top)}, \quad (4)$$

$$h_{\text{self}}(q) = d_{\text{self}}(q) - \varepsilon_{\text{self}}. \quad (5)$$

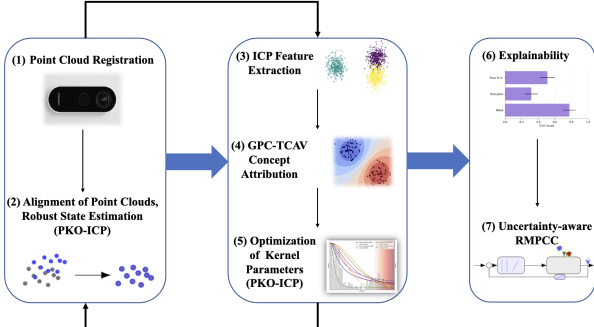


Fig. 2: Schematic description of *GUARD*.

Fig. 3: Overview of GUARD: concept-attributed perception drives risk-adaptive RMPCC in real time.

and

$$h_{\text{env},\ell}(q, p_{\text{obs}}) = d_{\text{env},\ell}(q, p_{\text{obs}}) - r_{\text{obs}} - \varepsilon_{\text{env}}$$

for each link  $\ell$ . Here,  $J_{ee}$  denotes the end-effector Jacobian;  $d_{\text{self}}$  and  $d_{\text{env},\ell}$  are the minimum distances to self-collision and to the  $\ell$ -th robot link's collision with the obstacle, respectively, as predicted by a deep neural network; and  $\varepsilon > 0$  denote safety margins. The optimization is solved via QP relaxation of the barrier inequalities via Jacobian linearization. The Gauss–Newton Hessian approximation enables real-time at 100 Hz. However, the method relies on a *perfectly accurate* perception. *GUARD* addresses this limitation via an uncertainty-aware ICP.

### III. THE FRAMEWORK *GUARD*

This section presents **GUARD** (Guided robot control via Uncertainty attribution and probAbilistic kernel optimization for Risk-aware Decision making) by combining and extending methods from prior works for safe robot systems. The following steps, illustrated in the figure 3, outline the complete *GUARD* pipeline:

- **Env. Perception:** Acquire RGB-D/LiDAR frames from the environment.
- **PKO-ICP:** Align point clouds, estimate pose  $T_k$  and residuals. PKO monitors the residual statistics.
- **Features from ICP:** Extract expressive point-cloud features (e.g., DGCNN or PointNet).
- **Kernel Optimization:** Proactively update the residual model and kernel hyperparameters via concept scores.
- **Explainability:** Generate per-concept reports of attribution and uncertainty over time.
- **Improved Control:** Feed uncertainty and attribution into the controller for safe movements.

#### A. Active PKO via Concept Feedback

*GUARD* optionally broadens the tuner to a vector  $\theta_k \in \Theta$  that may include a correspondence gate, robust-loss scale, measurement-noise, or length-scales additionally to the kernel scale. These additional parameters follow small regularized likelihood steps over a short residual window within safe bounds. Specifically, the PKO parameters are adapted online via the concept-level uncertainty of the TCAV-GPC module. *GUARD* initializes the parameter adaptation only if

necessary via the concepts that indicate *why* the estimate is uncertain. Small changes are introduced in directions that mitigate that cause. With the ICP pose  $T_k \in SE(3)$ , the residuals  $\{r_i\}$ , and the vector of registration parameters  $\theta_k \in \Theta$ , the TCAV-GPC module returns concept posteriors  $\pi_k = \{\pi_k(c)\}_{c \in \mathcal{C}}$  over  $\mathcal{C} = \{\text{noise, pose-error, overlap}\}$  and an accumulated uncertainty  $u_k$ . *GUARD* adapts the parameters once dominant concept and/or non-trivial uncertainty occur ( $\max_c \pi_k(c) \geq \tau_{\text{on}}$  and  $u_k \geq u_{\text{min}}$ ). If the condition is not met, parameters are held:  $\theta_{k+1} = \theta_k$ . *GUARD* refers to small mixed steps along concept-specific directions  $\{\mathbf{U}_c\}$ :

$$\Delta \theta_k = \eta_k s(u_k) \sum_{c \in \mathcal{C}} \alpha_c \pi_k(c) \mathbf{U}_c,$$

where  $\eta_k$  is a step size,  $s(u_k)$  scales the step with the accumulated uncertainty, and  $\alpha_c$  are per-concept gains. *GUARD* selects the exact schedules empirically. The updated parameters are projected onto the feasible set  $\Theta$ :

$$\theta_{k+1} = \Pi_{\Theta}(\theta_k + \Delta \theta_k).$$

If the control loop is close to its deadline, *GUARD* skips the adaptation and falls back to the uncertainty computation. If a dominant concept persists for several frames, *GUARD* varies the viewpoint. The computation  $O(|\mathcal{C}|d)$  is negligible compared to ICP and feature extraction.

#### B. Uncertainty-aware Robot Control

This section integrates the perception module into the RMPCC to relax the assumption on the perfectly accurate perception in [4]. Since uncertainties are proportional to risks, the perception uncertainty enables to develop risk-aware robot controllers: The scalar risk and per-concept posteriors modulate (i) the CBF relaxation (large slack penalties at high risk), (ii) collision margins and desired speed  $v_{\text{des}}$ , and (iii) soft weights  $w_c, w_l, w_o, w_{v_s}$  to trade efficiency for conservatism if perception uncertainty spikes. This preserves RMPCC's real-time capability with responsive safety margins to perception uncertainty. The perception module yields a risk measure  $\rho_k \in [0, 1]$  via concept posteriors and entropy

$$r_{\text{obs}}^{\text{eff}} = r_{\text{obs}} + \kappa_r \rho_k, \quad w_{v_s}^{\text{eff}} = w_{v_s} (1 - \kappa_v \rho_k). \quad (6)$$

## IV. EXPERIMENTS

#### A. Active PKO via Concept Feedback

The experiments evaluate standard point-to-plane ICP [17], Stein-ICP [21], and PKO-ICP [5] on a synthetic benchmark of geometric shapes (HELIX, TORUS, KNOT). Figure 4 summarizes the mean residuals. Also, one uncertainty source is injected for each run at randomized magnitudes.

**Runtime.** PKO-ICP attains a promising accuracy-latency trade-off, see Tab. I: Standard ICP runs at  $\sim 0.06$ – $0.15$  s (CPU) but with higher residuals; PKO-ICP achieves  $\sim 0.12$ – $0.35$  s (CPU) with lower residuals; Stein-ICP is most accurate but slower at  $\sim 0.80$ – $1.00$  s (GPU). PKO-ICP is significantly

TABLE I: Latency and mean residuals (approx.).

Method	Time/run	Helix	Torus	Knot
Std (CPU)	0.06–0.15 s	$\approx 0.25$	$\approx 0.30$	$> 0.80$
PKO (CPU)	0.12–0.35 s	$\approx 0.20$	$\approx 0.25$	$\approx 0.55$
Stein (GPU)	0.80–1.00 s	$\approx 0.15$	$\approx 0.20$	$\approx 0.30$

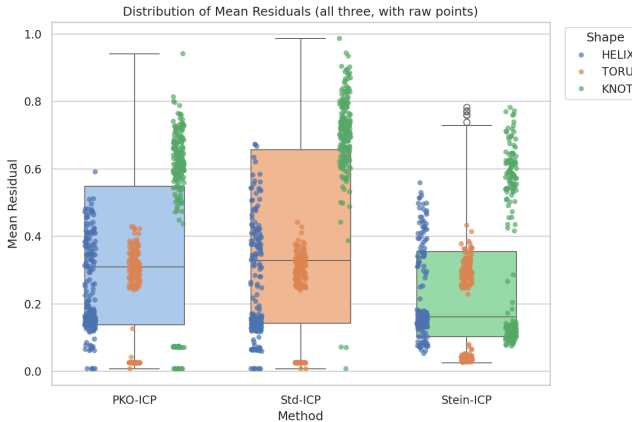


Fig. 4: Residual comparison under injected uncertainty. Distribution of mean residuals for standard ICP, PKO-ICP, and Stein-ICP on synthetic shapes (HELIX, TORUS, KNOT).

faster than Stein-ICP with comparable residuals and real-time capability.

**Shape-specific behavior.** As seen in Fig. 4 and Tab. I on HELIX, the average residuals are  $\sim 0.25/0.20/0.15$  (Standard/PKO/Stein). Thus, PKO reduces the mean residual by  $\sim 0.05$  vs. Standard and Stein yield  $\sim 0.05$  improvement. TORUS provides the same pattern. For the hardest KNOT, Standard ICP provides  $> 0.80$ , while PKO-ICP reduces it to  $\sim 0.55$  and Stein-ICP further to  $\sim 0.30$ .

**Concept attribution.** TCAV-GPC on PKO-ICP features provide uncertainty attributions. These attributions allow PKO updates to focus on the dominant cause, strengthening robustness while preserving efficiency.

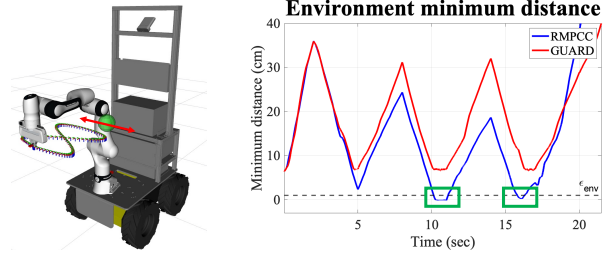
**OOD Robustness.** *GUARD* flags out-of-distribution frames using a reject rule on the calibrated uncertainty:

$$\text{OOD}_k = \mathbf{1} \left[ u_k > \tau_u \vee \max_{c \in \mathcal{C}} \pi_k(c) < \tau_p \right]. \quad (7)$$

On  $\text{OOD}_k=1$ , *GUARD* freezes kernel updates, set  $\rho_k \leftarrow 1$ , and reduces  $v_{\text{des}}^{\text{eff}}$  while inflating margins via (9). Thus,  $(\tau_u, \tau_p)$  are chosen on a small validation split to balance false positives vs. missed OOD events for conservatism.

### B. Uncertainty-aware Robot Control

The 7-DoF Panda manipulator Franka Emika was employed where the robot was given provided with a 3D lemniscate path shown in Figure 5a. The goal is to avoid a dynamic obstacle. When the obstacle is occluded or not detected, the baseline RMPCC assumes that the obstacle remains stationary at its last detected position. To replicate this in simulation, we enforced that at randomly chosen time intervals, the robot interpreted the detected obstacle as stationary for a certain duration, while in reality the obstacle continued to move. *GUARD* adjusts the obstacle's  $r_{\text{obs}}^{\text{eff}}$  and  $w_{v_s}$ , thereby enabling robust avoidance. Figure 5b illustrates  $d_{\text{env}} = \min_{\ell} d_{\text{env}, \ell}$ , the minimum distance between the robot and the obstacle over time. The baseline RMPCC neglects the distance between the detected and actual obstacle positions. Consequently, the min. distance falls below  $\varepsilon_{\text{env}}$ , resulting in a collision. In contrast, *GUARD* explicitly considers uncertainties, thereby yielding a robot movements.



(a) Setup

(b) Min. distance

Fig. 5: 7-DoF manipulator follows a 3D lemniscate with a dynamic obstacle; (a) setup; (b) minimum robot-obstacle distance for RMPCC (blue) and *GUARD* (red); dashed: safety margin  $\varepsilon_{\text{obs}}$ ; green boxes indicate collisions.

### C. Risk Mapping and Safety under Parameter Adaptation

*GUARD* collapses perception into a bounded risk  $\rho_k \in [0, 1]$ . The controller becomes conservative for high uncertainties. Calibrated concept posteriors  $\pi_k(c)$  and entropy  $u_k$  yield

$$\rho_k = \text{clip}_{[0,1]} \left( \beta_0 u_k + \sum_{c \in \mathcal{C}} \beta_c \pi_k(c) \right), \quad (8)$$

where  $\beta \geq 0$  weight each source. Larger  $\rho_k$  linearly inflates margins, increases slack penalty, and reduces speed:

$$r_{\text{obs}}^{\text{eff}} = r_{\text{obs}} + \kappa_r \rho_k, \quad \varepsilon_{\text{env}}^{\text{eff}} = \varepsilon_{\text{env}} + \kappa_{\varepsilon} \rho_k, \quad (9)$$

$$\gamma^{\text{eff}} = \gamma_0 + \kappa_{\gamma} \rho_k, \quad v_{\text{des}}^{\text{eff}} = v_{\text{des}} (1 - \kappa_v \rho_k). \quad (10)$$

This tightens the safe set and slows motion. *GUARD* clip/rate-limit  $\rho_k$  and cap slack via QP penalties via negligible runtime.

## V. LIMITATIONS

**Approximation Error and Barrier Shaping:** Jacobian linearization and the Gauss–Newton Hessian may degrade when kinematics or barriers vary sharply, leading to occasional solver overruns. The performance is sensitive to thresholds and class- $\mathcal{K}$  shaping in RBF( $\cdot$ ). Overly tight settings induce conservatism, while loose settings risk near-violations.

**PKO-TCAV limits:** The evaluation is limited in the diversity of scenarios and sensors. The sensitivity of the adaptation law to initialization, hyperparameters, and operating condition drift has not been studied. We plan broader ablation studies across kernel priors, update rates, and noise models.

**Closed-loop interactions.** Attribution-triggered active perception alters the sensing viewpoint and, indirectly, the control objective. This induces a switching closed-loop system. Stability, recursive feasibility, and absence of chattering necessitate analyses in future.

## VI. CONCLUSION

This paper presented *GUARD* that unifies traditional control RMPCC in [4] with learning-driven perception. *GUARD* combines the optimization of kernel parameters with uncertainty-aware perception to generate safe robot movements. The attributed risk adapts controller margins, yielding safety while preserving real-time performance. Experimental results demonstrate the performance and reliability of *GUARD*. Future work will complete the closed-loop integration of *GUARD* in real-world, fostering the evaluation with respect to safety standards.

## REFERENCES

[1] R. Tian, L. Sun, A. Bajcsy, M. Tomizuka, and A. D. Dragan, “Safety assurances for human-robot interaction via confidence-aware game-theoretic human models,” in *2022 International Conference on Robotics and Automation (ICRA)*. IEEE, 2022, pp. 11 229–11 235.

[2] O. Natan and J. Miura, “End-to-end autonomous driving with semantic depth cloud mapping and multi-agent,” *IEEE Transactions on Intelligent Vehicles*, vol. 8, no. 1, pp. 557–571, 2023.

[3] T. Miki, J. Lee, J. Hwangbo, L. Wellhausen, V. Koltun, and M. Hutter, “Learning robust perceptive locomotion for quadrupedal robots in the wild,” *Science Robotics*, vol. 7, no. 62, p. eabk2822, 2022. [Online]. Available: <https://www.science.org/doi/abs/10.1126/scirobotics.abk2822>

[4] J. Park, W.-J. Baek, and J. Yoon, “Reactive model predictive contouring control for robot manipulators,” 2025. [Online]. Available: <https://arxiv.org/abs/2508.09502>

[5] S. Choi and T.-W. Kim, “Probabilistic kernel optimization for robust state estimation,” *IEEE Robotics and Automation Letters*, vol. 10, no. 3, pp. 2998–3005, 2025.

[6] M. Elbanhawi and M. Simic, “Sampling-based robot motion planning: A review,” *IEEE Access*, vol. 2, pp. 56–77, 02 2014.

[7] S. Karaman and E. Frazzoli, “Sampling-based algorithms for optimal motion planning,” *The International Journal of Robotics Research*, vol. 30, no. 7, pp. 846–894, 2011. [Online]. Available: <https://doi.org/10.1177/0278364911406761>

[8] J. Schulman, Y. Duan, J. Ho, A. Lee, I. Awwal, H. Bradlow, J. Pan, S. Patil, K. Goldberg, and P. Abbeel, “Motion planning with sequential convex optimization and convex collision checking,” *The International Journal of Robotics Research*, vol. 33, no. 9, pp. 1251–1270, 2014. [Online]. Available: <https://doi.org/10.1177/0278364914528132>

[9] D. Rakita, B. Mutlu, and M. Gleicher, “RelaxedIK: Real-time synthesis of accurate and feasible robot arm motion,” in *Robotics: Science and Systems XIV*. Robotics: Science and Systems Foundation, jun 2018. [Online]. Available: <https://doi.org/10.15607%2Frss.2018.xiv.043>

[10] D. Nicolis, F. Allevi, and P. Rocco, “Operational space model predictive sliding mode control for redundant manipulators,” *Trans. Rob.*, vol. 36, no. 4, p. 1348–1355, Aug. 2020. [Online]. Available: <https://doi.org/10.1109/TRO.2020.2974092>

[11] Y. Wang, Y. Liu, M. Leibold, M. Buss, and J. Lee, “Hierarchical incremental mpc for redundant robots: A robust and singularity-free approach,” *Trans. Rob.*, vol. 40, p. 2128–2148, Jan. 2024. [Online]. Available: <https://doi.org/10.1109/TRO.2024.3370049>

[12] A. Romero, S. Sun, P. Foehn, and D. Scaramuzza, “Model predictive contouring control for time-optimal quadrotor flight,” *IEEE Transactions on Robotics*, vol. 38, no. 6, pp. 3340–3356, 2022.

[13] N. van Duijkeren, R. Verschueren, G. Pipeleers, M. Diehl, and J. Swovers, “Path-following nmpc for serial-link robot manipulators using a path-parametric system reformulation,” in *2016 European Control Conference (ECC)*, 2016, pp. 477–482.

[14] A. D. Ames, S. Coogan, M. Egerstedt, G. Notomista, K. Sreenath, and P. Tabuada, “Control barrier functions: Theory and applications,” in *2019 18th European Control Conference (ECC)*, 2019, pp. 3420–3431.

[15] A. Singletary, K. Klingebiel, J. Bourne, A. Browning, P. Tokumaru, and A. Ames, “Comparative analysis of control barrier functions and artificial potential fields for obstacle avoidance,” in *2021 IEEE/RSJ International Conference on Intelligent Robots and Systems (IROS)*, 2021, pp. 8129–8136.

[16] P. J. Besl and N. D. McKay, “A method for registration of 3-d shapes,” *IEEE Transactions on Pattern Analysis and Machine Intelligence*, vol. 14, no. 2, pp. 239–256, 1992.

[17] Y. Chen and G. Medioni, “Object modelling by registration of multiple range images,” *Image Vision Comput.*, vol. 10, no. 3, p. 145–155, Apr. 1992. [Online]. Available: [https://doi.org/10.1016/0262-8856\(92\)90066-C](https://doi.org/10.1016/0262-8856(92)90066-C)

[18] A. Censi, “An accurate closed-form estimate of icp’s covariance,” in *Proceedings 2007 IEEE International Conference on Robotics and Automation*, 2007, pp. 3167–3172.

[19] S. Bonnabel, M. Barczyk, and F. Goulette, “On the covariance of icp-based scan-matching techniques,” 2016. [Online]. Available: <https://arxiv.org/abs/1410.7632>

[20] D. Landry, F. Pomerleau, and P. Giguère, “Cello-3d: Estimating the covariance of icp in the real world,” in *2019 International Conference on Robotics and Automation (ICRA)*. IEEE Press, 2019, p. 8190–8196. [Online]. Available: <https://doi.org/10.1109/ICRA.2019.8793516>

[21] F. A. Maken, F. Ramos, and L. Ott, “Stein ICP for Uncertainty Estimation in Point Cloud Matching,” 2021. [Online]. Available: <https://arxiv.org/abs/2106.03287>

[22] B. Kim, M. Wattenberg, J. Gilmer, C. Cai, J. Wexler, F. Viegas, and R. sayres, “Interpretability beyond feature attribution: Quantitative testing with concept activation vectors (TCAV),” in *Proceedings of the 35th International Conference on Machine Learning*, ser. Proceedings of Machine Learning Research, J. Dy and A. Krause, Eds., vol. 80. PMLR, 10–15 Jul 2018, pp. 2668–2677. [Online]. Available: <https://proceedings.mlr.press/v80/kim18d.html>

[23] R. Q. Charles, H. Su, M. Kaichun, and L. J. Guibas, “Pointnet: Deep learning on point sets for 3d classification and segmentation,” in *2017 IEEE Conference on Computer Vision and Pattern Recognition (CVPR)*, 2017, pp. 77–85.

[24] Y. Wang, Y. Sun, Z. Liu, S. E. Sarma, M. M. Bronstein, and J. M. Solomon, “Dynamic graph cnn for learning on point clouds,” 2019. [Online]. Available: <https://arxiv.org/abs/1801.07829>

[25] Z. Qin, J. Lee, and R. Triebel, “Towards explaining uncertainty estimates in point cloud registration,” 2024. [Online]. Available: <https://arxiv.org/abs/2412.20612>